

MANY-BODY THEORY OF NUCLEAR AND NEUTRON STAR MATTER

V. R. PANDHARIPANDE, A. AKMAL and D. G. RAVENHALL

*Department of Physics, University of Illinois at Urbana-Champaign
1110 W. Green St., Urbana, Illinois 61801, USA*

Abstract

We present results obtained for nuclei, nuclear and neutron star matter, and neutron star structure obtained with the recent Argonne v_{18} two-nucleon and Urbana IX three-nucleon interactions including relativistic boost corrections. These interactions predict that matter will undergo a transition to a spin layered phase with neutral pion condensation. We also consider the possibility of a transition to quark matter.

1 Introduction

Properties of matter having densities up to ~ 1 nucleon/fm 3 are important in determining the structure and maximum mass of neutron stars. At such densities the average interparticle spacing is ~ 1 fm. It is well known that the rms charge radius of proton is ~ 0.8 fm, thus one may be concerned that nucleons 1 fm apart have too large a structural overlap, and may even cease to be nucleons. However, the large charge radius of protons is due to a diffuse cloud attributed to mesons. The charge form factor of the proton, as well as the magnetic form factors of the proton and the neutron are well approximated by the dipole form:

$$F(q) = (1 + q^2/q_0^2)^{-2}; \quad q_0 = 0.84 \frac{GeV}{c}. \quad (1)$$

The charge density obtained by inverting this form factor is:

$$\rho_{ch}(r) = 3.3 e^{-r/0.23} \text{ fm}^{-3}, \quad r \text{ in fm.} \quad (2)$$

The charge densities of two protons placed at ± 0.5 fm on the z-axis are shown in fig.1. We see that there is not too much structural overlap of protons 1 fm apart. We may therefore assume that they still are protons, and absorb the effects of the overlap into the two nucleon interaction. This assumption is supported by studies of the deuteron. The deuteron wave function peaks at

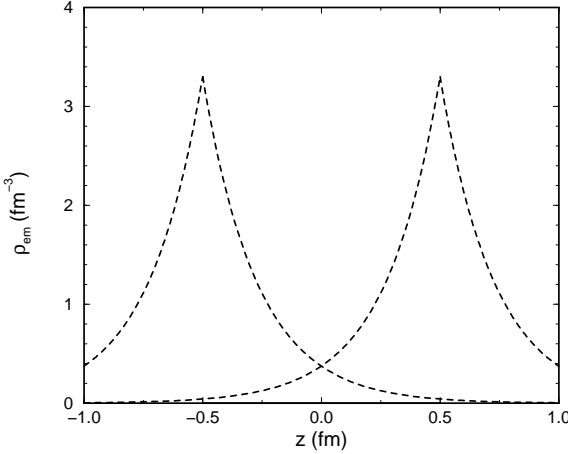


Figure 1: Charge density of two nucleons at $z = \pm 0.5$ fm, along the z-axis

~ 1 fm separation between the neutron and the proton in agreement with the observed deuteron form factors [1].

In nuclear many-body theory, nuclei and nuclear matter are described by the Hamiltonian:

$$H = \sum_i \frac{-\nabla^2}{2m} + \sum_{i < j} (v_{ij} + \delta v(\mathbf{P}_{ij})) + \sum_{i < j < k} V_{ijk}, \quad (3)$$

in which i, j, k, \dots denote nucleons. The first term is the nonrelativistic kinetic energy, and the second contains the two nucleon interaction v_{ij} in the center of mass frame of the interacting pair. The relativistic boost interaction $\delta v(\mathbf{P}_{ij})$ describes the dependence of two-nucleon interaction on their total center of mass momentum \mathbf{P}_{ij} , and the last term contains the three nucleon interaction. In principle the H can have additional terms, such as the boost correction for three-nucleon interaction, four nucleon interaction, *etc.*; however these terms are believed to have a negligible effect on neutron star structure. The above H describes only the hadronic part of neutron star matter which also contains electrons and, at high densities, muons to preserve charge neutrality and beta equilibrium. The relativistic kinetic energies of the leptons and the Coulomb interaction energies are to be added to the above hadronic H .

Recent developments in various terms of the nuclear Hamiltonian are discussed in the next section, while progress in the variational calculations of the properties of matter from this H is reviewed in sect. 3. The results for neutron

stars are given in sect. 4, while the possibility of a phase transition to quark matter is considered in sect. 5. A more detailed description of this work will be published elsewhere.

2 Modern Models of Nuclear Forces

In the early 1990's the Nijmegen group [2] carefully examined all the data on NN scattering at energies below 350 MeV published between 1955 and 1992. They extracted 1787 proton-proton and 2514 proton-neutron "reliable" data, and showed that these could determine all NN scattering phase shifts and mixing parameters quite accurately. NN interaction models which fit this Nijmegen data base with a $\chi^2/N_{data} \sim 1$ are termed "modern". These include the Nijmegen models [3] called Nijmegen I, II and Reid 93, the Argonne v_{18} [4] (A18) and CD-Bonn [5]. In order to fit both the proton-proton and neutron-proton scattering data simultaneously and accurately, these models include a detailed description of the electromagnetic interactions and terms that violate the isospin symmetry of the strong interaction via the differences in the masses of the charged and neutral pions, etc.

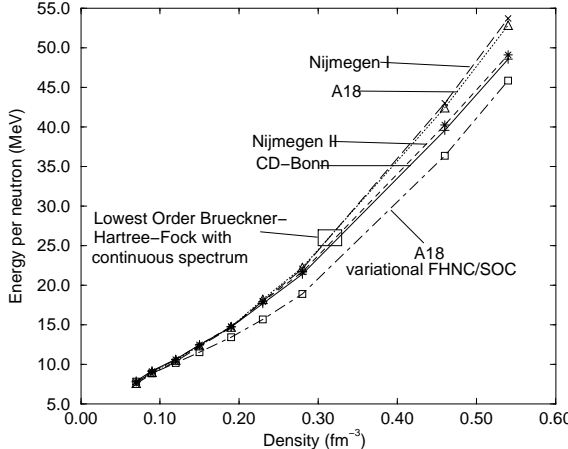


Figure 2: The $E(\rho)$ of neutron matter calculated from modern potential models. The upper four curves show results obtained with Brueckner-Hartree-Fock calculations, while the lower curve is with variational calculations.

In these five models the two nucleon interaction v_{ij} is expressed as a sum of the one-pion exchange potential v_{ij}^π and the rest of the interaction v_{ij}^R . They use different parameterizations of the v_{ij}^R , and the Nijmegen-I and CD-Bonn

also include nonlocalities suggested by boson-exchange representations. Thus, like the older models, they make different predictions for many-body systems. However, the differences in their predictions are much smaller than those between older models, presumably because they exactly fit the same large data set. For example, the triton ground state energies predicted by the modern Nijmegen and Argonne models, without the $\delta v(\mathbf{P}_{ij})$ and V_{ijk} terms in the Hamiltonian, are between -7.62 and -7.72 MeV [6], while that of CD-Bonn is -8.00 MeV [5]. This should be compared with the spread from -7.35 MeV (original Reid) to -8.35 MeV (Bonn-A) in the predictions of the older models. The predictions for the energies of dense neutron matter obtained from the modern potentials using lowest order Brueckner-Hartree-Fock (LOB) method [7] are also quite close together as shown in fig. 2. This figure also shows the energies of neutron matter calculated from the A18 potential by the variational method using chain summation techniques [8]. The difference between the results obtained for this modern potential using LOB and variational methods is larger than that in the results of all the modern potentials with the LOB method.

The modern potentials, like their predecessors, do not explain all of the observed nuclear properties. They all underbind the triton, and overpredict the density of nuclear matter. It is necessary to add three-nucleon (NNN) interactions to the Hamiltonian to reproduce these observables. The Urbana models of NNN interaction have only two terms:

$$V_{ijk} = V_{ijk}^{2\pi} + V_{ijk}^R, \quad (4)$$

the first gives the two-pion exchange NNN interaction via the pion-nucleon delta resonance [9], and its strength is denoted by the parameter $A_{2\pi}$; the second is a phenomenological spin-isospin independent, shorter range term with strength denoted by U_0 . The values of the parameters $A_{2\pi}$ and U_0 of the Urbana-IX (UIX) NNN potential are chosen such that in combination with A18 NN potential triton energy is reproduced via exact calculations and the equilibrium density of nuclear matter is reproduced via variational calculations [10]. The boost interaction $\delta v(\mathbf{P}_{ij})$ was negelected in these calculations to determine $A_{2\pi}$ and U_0 . Its effect is discussed later. It is unlikely that a combination of CD-Bonn and UIX potentials will reproduce the triton energy. Parameters of the NNN interaction have to refitted for each model of the NN interaction, as in the recent work of the Bochum group [11] using the Tucson-Melbourne [12] model of $V_{ijk}^{2\pi}$. The fitted V_{ijk} then partly corrects for the deviation of the model v_{ij} from its exact representation. We hope that predictions of the modern combinations of v_{ij} and V_{ijk} will be significantly less

Table 1: Results of Quantum Monte Carlo Calculations in MeV

A_Z	$(J^\pi; T)$	v_{ij}^π	$V_{ijk}^{2\pi}$	v_{ij}^R	V_{ijk}^R	E_{GFMC}	$\Delta E_{expt.}$	ΔE_{VMC}
2_H	$(1^+; 0)$	-21.3	0	-0.8	0	-2.22	0	0
3_H	$(\frac{1}{2}^+; \frac{1}{2})$	-43.8	-2.2	-14.6	1.0	-8.47	-0.01(1)	0.15
$^4_{He}$	$(0^+; 0)$	-99.4	-11.7	-36.0	5.3	-28.30	0.00(2)	0.52
$^6_{He}$	$(0^+; 1)$	-109	-13.6	-56	6.4	-27.64	-1.63(14)	2.8
$^6_{Li}$	$(1^+; 0)$	-129	-13.5	-50	6.3	-31.25	-0.74(11)	3.2
$^7_{He}$	$(\frac{3}{2}^-; \frac{3}{2})$	-110	-14.1	-61	6.7	-25.2	-3.7(2)	4.7
$^7_{Li}$	$(\frac{3}{2}^-; \frac{1}{2})$	-153	-17.1	-68	8.2	-37.4	-1.8(3)	4.7
$^8_{He}$	$(0^+; 2)$	-121	-15.8	-74	7.5	-25.8	-5.6(6)	6.1
$^8_{Li}$	$(2^+; 1)$	-157	-22.2	-104	11.0	-38.3	-3.0(6)	8.6
$^8_{Be}$	$(0^+; 0)$	-224	-28.1	-72	13.3	-54.7	-1.8(6)	6.6

model dependent than those of the v_{ij} alone.

It has recently become possible to calculate all the bound states of up to eight nucleons from realistic nuclear forces with the Greens Function Monte Carlo (GFMC) method. Since solar and primodial fusion reactions primarily involve nuclei having $A \leq 8$, they have a special role in the universe. Here we use the results obtained with A18, without $\delta v(\mathbf{P}_{ij})$, and UIX interactions to test the accuracy of variational wave functions and the interaction models. The calculated energies from [10] and [13] are listed in Table I. Its first two columns specify the nuclear state and the next four give the calculated expectation values of the interaction components. The last three columns list the energy calculated with GFMC, the difference between the experimental and GFMC energies, and that between our optimum variational and GFMC energies. The v_{ij}^π seems to give the dominant contribution to nuclear binding, while v_{ij}^R is also essential for all but the deuteron. There is a large cancellation between the kinetic and two-nucleon interaction contributions, causing the total nuclear energy to be much smaller than the $\langle v_{ij} \rangle$. The $\langle V_{ijk}^{2\pi} \rangle$ is much smaller than $\langle v_{ij}^\pi \rangle$; however, it is a significant fraction of the nuclear binding energy. The $\langle V_{ijk}^R \rangle$ is the smallest, and $\Delta E_{expt.}$, the difference between experiment and theory is even smaller. In the neutron rich nuclei $^7_{He}$ and $^8_{He}$, the $\Delta E_{expt.}$ is comparable to the $\langle V_{ijk}^R \rangle$, indicating that the UIX model may not be describing the interaction between three neutrons very well. All the p-shell nuclei having $A > 5$ are underbound, and the problem increases with the magnitude of nuclear isospin T. New models of V_{ijk} are being studied to reduce the $\Delta E_{expt.}$.

Table 1 also reveals another problem; the difference ΔE_{VMC} between GFMC

and variational Monte Carlo (VMC) energies is surprisingly large in the p-shell nuclei. Earlier successes in variational calculations of the $A \leq 4$ s-shell nuclei led to hopes that the variational calculations of larger nuclei and uniform nucleon matter, using cluster expansions [14], and chain summation methods [8] may have less than 10 % errors. The present VMC for ${}^8\text{Be}$, which includes many three-body correlations omitted in variational calculations of larger nuclei and uniform matter, has a 12 % error. It appears that important aspects of the wavefunctions of p-shell nuclei are still not understood.

All NN interaction models are obtained by fitting NN scattering data in the center of mass frame. The model v_{ij} denotes the interaction between two nucleons in the frame in which their total momentum $\mathbf{P}_{ij} = \mathbf{p}_i + \mathbf{p}_j$, is zero. In the rest frame of all nuclei other than the deuteron, the \mathbf{P}_{ij} of a pair of nucleons is non-zero. One then has to use the correct NN interaction:

$$v(\mathbf{P}_{ij}) = v_{ij} + \delta v(\mathbf{P}_{ij}), \quad (5)$$

between particles with total momentum \mathbf{P}_{ij} . The correction $\delta v(\mathbf{P}_{ij})$ is called the boost interaction [15]; it is zero when $\mathbf{P}_{ij} = 0$.

It is useful to consider a familiar example. The Breit interaction [16] between two particles of mass m and charge Q is, ignoring spin dependent terms for brevity, given by:

$$\frac{Q^2}{r_{ij}} \left(1 - \frac{\mathbf{p}_i \cdot \mathbf{p}_j}{2m^2} - \frac{\mathbf{p}_i \cdot \mathbf{r}_{ij} \mathbf{p}_j \cdot \mathbf{r}_{ij}}{2m^2 r_{ij}^2} \right), \quad (6)$$

which depends upon both \mathbf{p}_i and \mathbf{p}_j . We can express it in our notation as a sum of v_{ij} and $\delta v(\mathbf{P}_{ij})$:

$$v_{ij} = \frac{Q^2}{r_{ij}} \left(1 + \frac{p_{ij}^2}{2m^2} + \frac{(\mathbf{p}_{ij} \cdot \mathbf{r}_{ij})^2}{2m^2 r_{ij}^2} \right), \quad (7)$$

$$\delta v(\mathbf{P}_{ij}) = - \frac{Q^2}{r_{ij}} \left(\frac{P_{ij}^2}{8m^2} + \frac{(\mathbf{P}_{ij} \cdot \mathbf{r}_{ij})^2}{8m^2 r_{ij}^2} \right), \quad (8)$$

where $\mathbf{p}_{ij} = (\mathbf{p}_i - \mathbf{p}_j)/2$, is the relative momentum. The dependence of v_{ij} on \mathbf{p}_{ij} is included in all modern models, however, the $\delta v(\mathbf{P}_{ij})$ has been neglected in the majority of nuclear and neutron star calculations.

Following the work of Krajcik and Foldy [17], Friar [18] obtained the following equation relating the boost interaction of order P^2 to the interaction in the center of mass frame:

$$\delta v(\mathbf{P}) = - \frac{P^2}{8m^2} v + \frac{1}{8m^2} [\mathbf{P} \cdot \mathbf{r} \mathbf{P} \cdot \nabla, v] + \frac{1}{8m^2} [(\sigma_i - \sigma_j) \times \mathbf{P} \cdot \nabla, v]. \quad (9)$$

The general validity of this equation in relativistic mechanics and field theory was recently discussed [15]. Nonrelativistic Hamiltonians containing boost interactions include all terms quadratic in the particle velocities. The contribution of the two-body boost interaction to the energy of light nuclei has been evaluated with VMC method [19, 20, 21]; it is repulsive and equals $\sim 37\%$ of that of V_{ijk}^R listed in Table 1. Therefore about 37 % of the V_{ijk}^R in UIX simulates the contribution of the neglected δv . The three-nucleon interaction to be used in Hamiltonians containing δv is denoted by V_{ijk}^* ; the strength of V_{ijk}^{*R} is 0.63 times that of V_{ijk}^R in UIX, while $V_{ijk}^{*2\pi} = V_{ijk}^{2\pi}$. In nuclei and in nuclear matter at densities up to ~ 0.2 nucleons/fm³ Hamiltonians containing $V^* + \delta v$ and V alone give rather similar results, but at higher densities they differ substantially. Naturally the results of the Hamiltonian with $V^* + \delta v$ are more reliable.

One can also consider relativistic nuclear Hamiltonians of the type:

$$H_R = \sum \sqrt{p_i^2 + m^2} + \sum (\tilde{v}_{ij} + \delta v(\mathbf{P}_{ij})) + \sum \tilde{V}_{ijk} + \dots, \quad (10)$$

where $\tilde{v}, \tilde{V}, \dots$ include relativistic nonlocalities [21], and the boost interactions include terms of higher order in \mathbf{P}_{ij} . We must refit the two-nucleon scattering data to determine the \tilde{v} in H_R , using relativistic kinetic energies [19, 21]. Uncorrelated nucleons in nuclei have small momenta of order $m/4$, thus the correction to their nonrelativistic kinetic energy is negligible. However, due to correlations induced by the strong \tilde{v} , a pair of nucleons acquire large relative momenta at small r_{ij} . The results obtained for light nuclei with H_R and the H given by eq.(3) are very similar [21], indicating that substantial improvements are obtained by including the relativistic boost interactions in the nonrelativistic Hamiltonian, as is well known for electromagnetic interactions.

3 Dense Nucleon Matter

The equation of state (EOS) of cold symmetric nuclear matter (SNM) and pure neutron matter (PNM) has been recently calculated with the variational method using chain summation techniques [8, 22]. Calculations have been done with the Hamiltonians with and without boost interactions.

We will first discuss the results presented in ref. [8] for the Hamiltonian without boost interactions. The calculated SNM and PNM energies are shown in figs.3 and 4 along with the results of earlier calculations [23, 24]. The density dependence of the U-DDI interaction was chosen to obtain the empirical saturation properties of SNM, so the minimum of that curve may be regarded

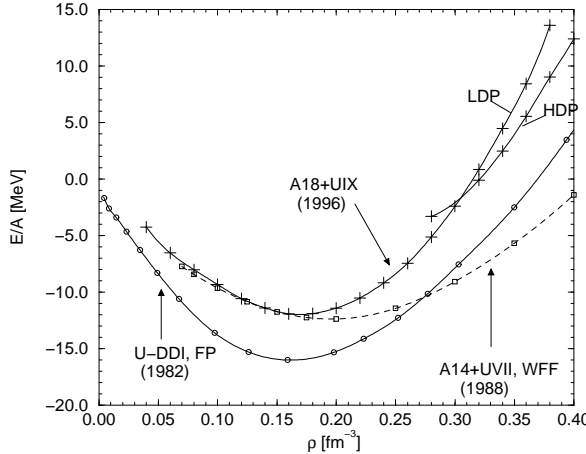


Figure 3: $E(\rho)$ of SNM calculated from A18 and UIX interactions compared with the results of earlier calculations. The two sets of variational minima obtained at $\rho > 0.28/fm^3$ are labeled LDP and HDP for low and high density phases.

as experimental data. The calculated energy of -12 MeV/A is higher than the observed -16 MeV/A. However we now believe that much of this difference is due to the simplicity of the variational wave functions used in nucleon matter calculations. Use of improved variational wave functions should lower the SNM energy by more than two MeV/A. Comparison of VMC and GFMC results for energies of eight neutrons bound in a weak potential well [25] indicate that the present variational wave functions are more accurate for PNM than for SNM.

The calculated energies indicate a phase transition in SNM at a density of $\sim 0.3/fm^3$ (fig.3) and in PNM at $\sim 0.2/fm^3$ (fig.4). Detailed analysis of the pair distribution functions and sums of response functions [8] indicate that the phase at higher densities has spin-isospin order expected from neutral pion condensation, first considered by Migdal [26]. The variational wave functions used in this study are appropriate for isotropic matter. The phase transition is signaled by a change in the range and strength of tensor correlations. It is likely that the phase at higher density will be better described with a liquid crystal wave function with alternating spin layers [27] used in many studies with effective interaction models.

As realized long ago by Migdal, this transition is very sensitive to the short range behavior of the $\sigma_i \cdot \sigma_j$ and $\sigma_i \cdot \sigma_j \tau_i \cdot \tau_j$ interactions between nucleons. It did not occur in either SNM or PNM with the Urbana v_{14} model of 1981,

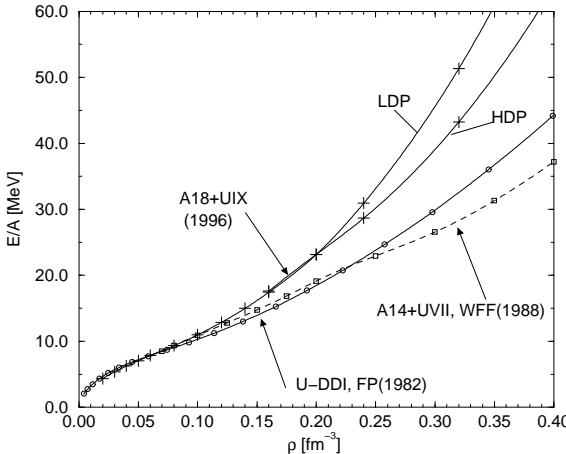


Figure 4: $E(\rho)$ of PNM. See fig.3 caption for details.

while it occurred only in PNM with the later Argonne v_{14} model of 1984. The Urbana-Argonne potentials have similar forms, but are fit to different data sets. The 1981 (1984) Urbana (Argonne) v_{14} models were fit to the n-p phase shifts available in the late 1970's (early 1980's), while the A18 is fit directly to the Nijmegen 1994 p-p and n-p scattering data base. The quality of the fit obtained by the A18 potential is much higher, and thus it is likely that it provides a more accurate representation of the nuclear force. The pion exchange part, $V_{ijk}^{2\pi}$, of the three-nucleon interaction is essential for the transition to occur in SNM, while in PNM it occurs at a much higher density in the absence of V_{ijk} .

The composition of nucleon matter energy calculated from A18 and UIX interactions is listed at selected densities in table 2, in which T-1B denotes the Fermi gas kinetic energy. The v-2B-S and T-2B-S list the two-body (2B) cluster contributions to the potential and kinetic energy from the static parts of the pair interaction and correlation operators. The v-2B-MD and T-2B-MD show 2B contributions having one or more momentum dependent (MD) interaction or correlations. These are conveniently regarded as the difference between the total 2B energies and their static parts. The static many-body (MB) contributions, MB-S, as well as the expectation values of the three-nucleon interactions are calculated with the Fermi hypernetted and single operator chain summation methods, presumably quite accurately. However, the MB contributions containing MD interaction or correlations, as well as the boost interaction $\delta v(\mathbf{P}_{ij})$, are evaluated from dressed three-body clusters. The δE -2B lists an estimate of the change in energy that may be obtained by allowing additional

Table 2: Composition of nucleon matter energy in MeV.

Type	SNM	SNM	SNM	SNM	PNM	PNM	PNM	PNM
$\rho(fm^{-3})$	0.08	0.16	0.32	0.64	0.08	0.16	0.32	0.64
T-1B	13.9	22.1	35.1	55.7	22.1	35.1	55.7	88.4
v-2B-S	-36.5	-66.7	-117.9	-227.2	-26.7	-49.4	-93.0	-185.7
T-2B-S	10.0	20.3	37.5	74.1	7.4	13.1	24.9	44.8
v-2B-MD	0.4	2.1	9.4	28.6	1.3	3.9	18.0	53.3
T-2B-MD	0.2	0.6	1.9	5.4	1.1	2.8	10.9	35.6
MB-S	3.4	5.5	9.2	25.6	3.2	6.4	1.8	-9.0
MB-MD	0.7	3.2	13.4	61.7	0.1	1.1	14.2	60.1
$V_{ijk}^{2\pi}$	-0.8	-3.6	-13.3	-82.0	0.3	1.2	-17.4	-76.9
V_{ijk}^{*R}	0.9	4.0	19.4	98.2	0.5	2.8	19.3	101.0
$\delta v(\mathbf{P}_{ij})$	0.6	2.1	6.4	21.0	0.7	2.2	6.9	21.5
δE -2B	-0.6	-1.8	-5.2	-9.2	-0.8	-1.3	-2.5	-5.5
Total E	-8.0	-12.2	-4.2	58.4	9.7	17.9	38.8	127.6

flexibility in the two-body correlations. We note that at high densities the MD parts, the V_{ijk}^* and $\delta v(\mathbf{P}_{ij})$ give significant contributions.

4 Neutron Star Matter

The matter at subnuclear densities in the outer and inner crusts of neutron stars has interesting structures as discussed at this meeting by Pethick and Ravenhall [28, 29]. Here we focus on the matter below the crust assuming that it is a uniform mixture of neutrons, protons, electrons and muons in beta equilibrium. The calculated energies of SNM and PNM are fitted by generalized Skyrme type effective interactions [30] having different parameters below and above the pion condensation phase transition. The beta equilibrium conditions are calculated from these effective interactions.

Ignoring mixed phase regions the normal matter at density and proton fraction of $0.204 fm^{-3}$ and 0.073 is found to be in equilibrium with pion condensed matter at $0.237 fm^{-3}$ and 0.057 for our most reliable model with boost and three-nucleon interactions. Obviously the matter in the phase with pion condensation has a lower charge density than the matter without condensation. Therefore, in reality the transition will proceed through mixed phase regions of the type discussed by Glendenning [31] and Heiselberg *et. al.* [32] in the context of the transition from hadronic to quark matter. The mixed phase regions in the pion condensation transition do not seem to have a large effect on

the structure of neutron stars because the discontinuity in the charge density is rather small. For example, the predicted thickness of the mixed phase regions varies from ~ 40 to 14 m in stars with 1.41 to $2.1 M_{\odot}$; however these predictions are quite crude because our calculations of the pion condensed phase are still incomplete.

The calculated density dependence of the proton fraction in neutron star matter is shown in fig.5 for the Hamiltonians containing only A18, A18+ δv , A18+ δv +UIX*, and A18+UIX interactions. The earlier results obtained with the U-DDI interaction (FPS) are shown for comparison. Both the boost and the three nucleon interactions increase the proton fraction in matter, but it remains below the critical value of 0.148 needed for direct Urca cooling, in the range of neutron star densities. The plus signs in fig.5 show the proton fractions calculated with the A18 interaction alone with the LOB method [7]. These are in reasonable agreement with the results of our calculations up to a density of 0.6 fm^{-3} . The density dependence of the electron chemical potential in matter is shown in fig.6.

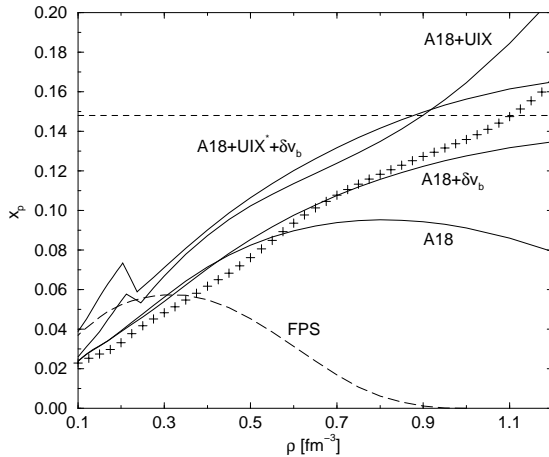


Figure 5: The proton fraction in matter in beta equilibrium for various model Hamiltonians. The plus signs show the results obtained for the A18 Hamiltonian with LOB method.

The predicted neutron star properties appear in figures 7 and 8. The dotted lines in these figures show results obtained using the PNM EOS. They are not very different from those obtained with matter in beta equilibrium. Due to the presence of momentum dependent and three-nucleon interactions in the present nuclear Hamiltonians, the predicted sound velocity in matter

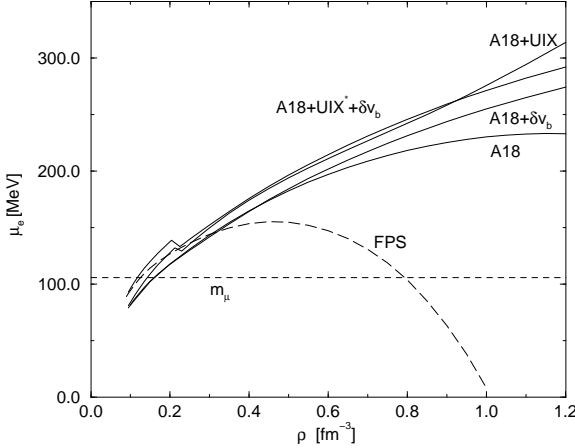


Figure 6: The electron chemical potential in neutron star matter for various model Hamiltonians. Matter contains muons when μ_e exceeds the muon mass m_μ .

can exceed the velocity of light. The densities at which superluminal sound occurs in each model are marked by vertical bars in fig.7. These densities are very close to the maximum densities that can occur in neutron stars, therefore limiting the the velocity of sound to be $\leq c$ does not have a significant effect on the predicted maximum masses.

Observations of binary neutron stars have confirmed the existence of $1.4 M_\odot$ neutron stars allowed by all models. Recently several authors [33, 34, 35] have argued that there are indications of the existence of neutron stars with $M \sim 2M_\odot$, which would rule out models without three-body forces, but see ref. [36] and Lamb's contribution [37].

5 Transition to Quark Matter

It is expected that at some large density there will be a transition from nucleon matter to quark matter (QM). Several authors [38] have studied the energy of cold QM using the Bag-model, in which the total energy density contains a “Bag-constant” B , that takes into account the difference between the energies of the physical and QM vacua, and the energy of quarks interacting via one gluon exchange interaction calculated in first order of α_s . The u and d quarks are assumed to be massless, and mass of s quarks is taken as 150 MeV. The energy density of QM obtained with $B = 122$ and 200 MeV/fm 3 is compared

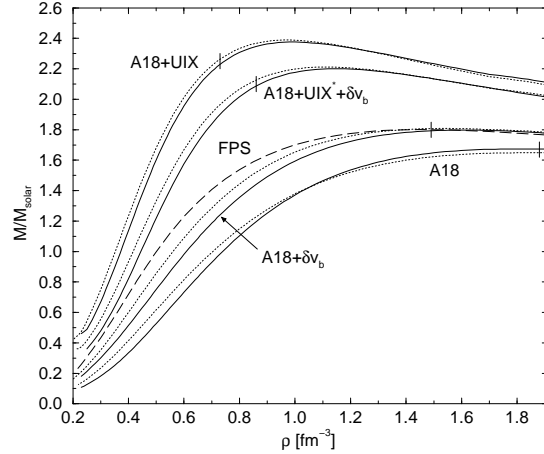


Figure 7: The dependence of neutron star mass on its central density for various model Hamiltonians. The full (dotted) lines show results obtained with the EOS of matter in beta equilibrium (PNM), and the vertical bars show where matter becomes superluminal in these models.

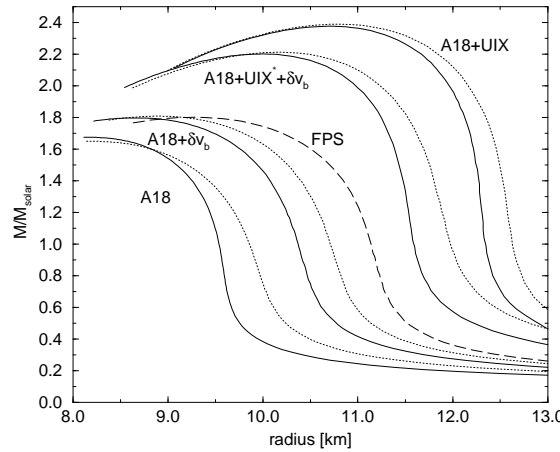


Figure 8: Neutron star mass-radius relation obtained from various model Hamiltonians. See caption of fig.7 for notation.

with that of nucleon matter (NM) in beta equilibrium for the more realistic models containing boost interaction, in fig. 9. The value $B = 122 \text{ MeV/fm}^3$ is supported by an analysis using the average of nucleon and delta-resonance masses [39]. In the absence of three-body interactions NM is found to have lower energy than QM up to a large density of $\sim 1.6 \text{ fm}^{-3}$. However, the transition density is lowered to $\sim 1 \text{ fm}^{-3}$ after including the contributions of the three nucleon interaction.

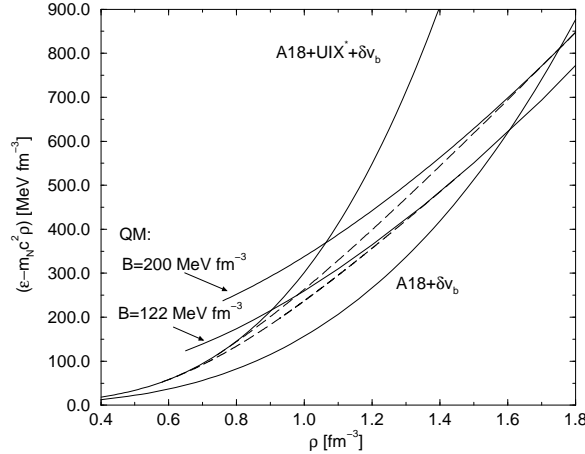


Figure 9: The energy densities of electrically neutral QM and NM are shown by full lines, while the dashed lines show those for matter with mixed QM and NM phases.

Glendenning [31] realized that it is not necessary to require the QM and NM phases to be separately charge neutral; a mixture of NM and QM can exist in a uniform lepton gas. Neglecting the energy of the interface between the QM and NM, and using the $A18 + \delta v + \text{UIX}^*$ model of NM, the transition occurs over the density range $\rho = 0.74$ to 1.80 fm^{-3} for $B = 200$, and 0.58 to 1.46 fm^{-3} for $B = 122 \text{ MeV/fm}^3$. At the lower end of this density range we have mostly NM with drops of QM, while at the higher end we will have mostly QM with drops of NM [32].

The dependence of the mass of neutron stars on their central density, obtained after including the effects of the transition to quark matter on the EOS are shown in fig.10. For $B = 122 \text{ MeV/fm}^3$ and the $A18 + \delta v + \text{UIX}^*$ NM Hamiltonian stars with masses above $1.5 M_\odot$ seem to have drops of quark matter in their cores. The maximum mass is reduced to $\sim 1.9 M_\odot$ corresponding to a central density of $\sim 1.1 \text{ fm}^{-3}$. In this model pure quark matter appears at

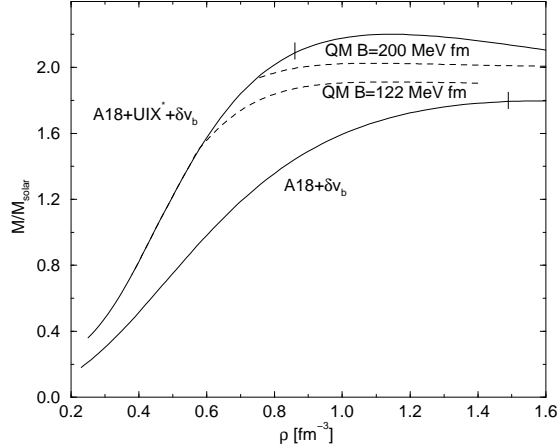


Figure 10: Dependence of neutron star mass on its central density. Full lines show results obtained with NM EOS, while dashed lines show results obtained after including the effect of the transition to QM on the EOS.

$\rho = 1.46 \text{ fm}^{-3}$; therefore even the most massive stars have mixed QM and NM phases in their interior. On the other hand, if $B = 200 \text{ Mev/fm}^3$ the maximum mass becomes $\sim 2M_{\odot}$, and stars with masses from 1.93 to $2.01 M_{\odot}$ have quark drops in their interior.

Acknowledgments

We would like to thank A. Arriaga, G. Baym, J. Carlson, J. Forest, H. Heiselberg, C. J. Pethick, S. C. Pieper, R. Schiavilla, E. F. Staubo and R. B. Wiringa for many of the results discussed here, and M. Hjorth-Jensen for communicating the results of neutron matter calculations. This work has been partly supported by the US National Science Foundation under Grant PHY94-21309.

References

- [1] J. L. Forest, V. R. Pandharipande, S. C. Pieper, R. B. Wiringa, R. Schiavilla and A. Arriaga, Phys. Rev. C **54**, 646 (1996).
- [2] V. G. J. Stoks, R. A. M. Klomp, M. C. M. Rentmeester and J. J. de Swart, Phys. Rev. C **48**, 792 (1993).

- [3] V. G. J. Stoks, R. A. M. Klomp, C. P. F. Terheggen and J. J. de Swart, Phys. Rev. C **49**, 2950 (1994).
- [4] R. B. Wiringa, V. G. J. Stoks and R. Schiavilla, Phys. Rev. C **51**, 38 (1995).
- [5] R. Machleidt, F. Sammarruca and Y. Song, Phys. Rev. C **53**, R1483 (1996).
- [6] J. L. Friar, G. L. Payne, V. G. J. Stoks and J. J. de Swart, Phys. Lett. B **311**, 4 (1993).
- [7] L. Engvik, M. Hjorth-Jensen, R. Machleidt, H. Muther and A. Polls, Nucl. Phys. (1997) to be published.
- [8] A. Akmal and V. R. Pandharipande, Phys. Rev. C **56**, 2261 (1997).
- [9] J. Fujita and H. Miyazawa, Prog. Theo. Phys. **17**, 360 (1957).
- [10] B. S. Pudliner, V. R. Pandharipande, J. Carlson, S. C. Pieper and R. B. Wiringa, Phys. Rev. C **56**, 1720 (1997).
- [11] W. Glockle, private communication (1997).
- [12] S. A. Coon, M. D. Scadron, P. C. McNamee, B. R. Barrett, D. W. E. Blatt and B. H. J. McKellar, Nucl. Phys. A **317**, 242 (1979).
- [13] R. B. Wiringa, Proc. of XV th Int. Conf. on Few Body Problems, (1997) to be published
- [14] S. C. Pieper, R. B. Wiringa and V. R. Pandharipande, Phys. Rev. C **46**, 1741 (1992).
- [15] J. L. Forest, V. R. Pandharipande and J. L. Friar, Phys. Rev. C **52**, 568 (1995).
- [16] H. A. Bethe and E. E. Salpeter, *Quantum mechanics of one and two electron atoms*, page 170, Academic Press (1957).
- [17] R. A. Krajcik and L. L. Foldy, Phys. Rev. D **10**, 1777 (1974).
- [18] J. L. Friar, Phys. Rev. C **12**, 695 (1975).
- [19] J. Carlson, V. R. Pandharipande and R. Schiavilla, Phys. Rev. C **47**, 484 (1993).

- [20] J. L. Forest, V. R. Pandharipande, J. Carlson and R. Schiavilla, Phys. Rev. C **52**, 576 (1995).
- [21] J. L. Forest, University of Illinois Ph. D. Thesis (1997).
- [22] A. Akmal, V. R. Pandharipande and D. G. Ravenhall, Phys. Rev. C, to be published (1998).
- [23] B. Friedman and V. R. Pandharipande, Nucl. Phys. A **361**, 501 (1981).
- [24] R. B. Wiringa, V. Fiks and A. Fabrocini, Phys. Rev. C **38**, 1010 (1988).
- [25] B. S. Pudliner, A. Smerzi, J. Carlson, V. R. Pandharipande, S. C. Pieper and D. G. Ravenhall, Phys. Rev. Lett. **76**, 2416 (1996).
- [26] A. B. Migdal, Rev. Mod. Phys. **50**, 107 (1978).
- [27] T. Kunihiro, T. Muto, T. Takatsuka, R. Tamagaki and T. Tatsumi, Prog. Theor. Phys. Suppl. **112** (1993).
- [28] C. J. Pethick and D. G. Ravenhall, in these proceedings.
- [29] C. J. Pethick and D. G. Ravenhall, Ann. Rev. Nuc. Par. Sci. **45**, 429 (1995).
- [30] V. R. Pandharipande and D. G. Ravenhall, Proc. NATO Adv. Res. Workshop on Nuclear Matter and Heavy Ion Collisions, Les Houches, ed. M. Soyeur et. al., Plenum, New York, 103 (1989).
- [31] N. K. Glendenning, Phys. Rev. D **46**, 1274 (1992).
- [32] H. Heiselberg, C. J. Pethick and E. F. Staubo, Phys. Rev. Lett. **70**, 379 (1993).
- [33] M. H. van Kerkwijk, P. Bergeron and S. R. Kulkarni, Ap. J. **467**, L89 (1996).
- [34] P. Kaaret, E. C. Ford and K. Chen, Ap. J. **480**, L27 (1997).
- [35] W. Zhang, T. E. Strohmayer and J. H. Swank, Ap. J. **482**, L167 (1997).
- [36] M. C. Miller, F. K. Lamb and D. Psaltis, Ap. J. in press
- [37] F. K. Lamb, in these proceedings.

- [38] B. Freedman and L. McLerran, Phys. Rev. D **17**, 1107 (1978).
- [39] J. Cleymans, R. V. Gavai and E. Suhonen, Phys. Rept. **130**, 217 (1986).